

Fast state and trap rotation of a particle in an anisotropic potential

I. Lizuain

Department of Applied Mathematics, University of the Basque Country UPV/EHU,
Donostia-San Sebastián, Spain

E-mail: ion.lizuain@ehu.eus

A. Tobalina

Department of Physical Chemistry, University of the Basque Country UPV/EHU,
Apdo. 644, Bilbao, Spain

A. Rodriguez-Prieto

Department of Applied Mathematics, University of the Basque Country UPV/EHU,
Bilbao, Spain

J. G. Muga

Department of Physical Chemistry, University of the Basque Country UPV/EHU,
Apdo. 644, Bilbao, Spain

Abstract. We study the dynamics of a quantum or classical particle in a two-dimensional rotating anisotropic harmonic potential. By a sequence of symplectic transformations for constant rotation velocity we find uncoupled normal generalized coordinates and conjugate momenta in which the Hamiltonian takes the form of two independent harmonic oscillators. The decomposition into normal-mode dynamics enables us to design fast trap-rotation processes to produce a rotated version of an arbitrary initial state, when the two normal frequencies are commensurate.

Submitted to: *J. Phys. A: Math. Theor.*

1. Introduction

Motivated by existing or developing quantum technologies, much work is currently being devoted to control the motional dynamics of quantum systems. Basic operations such as shuttling, expansions/compressions, merging and separation of atom or ion chains, or rotations of the quantum states are needed to implement interferometers, quantum information applications, or quantum thermodynamical devices. Performing fast operations that do not leave residual excitations is generically of interest not only to save time but to avoid decoherence as well.

Shortcuts to adiabaticity (STA) are proposed as a set of efficient techniques to design such operations [1, 2]. For two or more effective dimensions, shortcut design, by inverse engineering the control parameters using invariants of motion, is much facilitated by finding *dynamical normal modes* [3]. These modes are independent harmonic motions in the regime of small oscillations corresponding in general to time-dependent harmonic oscillators. Studies on different operations on trapped ions [4, 3, 5, 6, 7, 8, 9] made clear that it is not always possible to find a point transformation (a transformation in which the new coordinates only depend on the old ones and not on old momenta) that leads to independent normal modes. The condition that allows to find a point transformation was finally given in [10] for two-dimensional (2D) Hamiltonians: the effective potential can be scaled or translated but it should not rotate. Thus the rotation of a 2D anisotropic trap is the paradigmatic model in which such point transformation cannot be made and it was left as an open question if more general transformations could be used to speed up the rotation [10]. The inertial effect due to the trap rotation can be formally compensated by an effective angular momentum term [11, 10] to leave the particle at rest in the rotating frame. This term though may be difficult to implement, for example if the particle is not charged, so we consider in this paper that the only manipulation available is the rotation of the trap itself, without any additional force. STA for simple 1D-trap rotations, without compensation terms, were described in [8] but STA for the more realistic 2D anisotropic trap had not been described.

The goal of this work is to perform a rotation as represented schematically in Fig. 1 in the lab frame of coordinates x, y : The trap is at rest for $t < 0$; then it is rotated up to time T ; and finally it remains again at rest for $t > T$. The trap rotation must be designed such that the state at time T is exactly the rotated version of the initial state at time $t = 0$, *for all possible initial states*. Equivalently, from the point of view of the rotating frame, the objective is to get at time T the same state that was prepared at time 0, regardless of what that state may be.

Rotations of condensates or of a few particles are of interest for different reasons, such as reordering chains, redirecting, squeezing [8], or creating artificial magnetism [12, 13]. Here we treat the simplest case of a single particle in a rotating 2D trap. The operation would be instrumental in driving atoms through corners and junctions in a scalable quantum processor [15, 14], and may be regarded as a first step towards the more difficult problem of rotating ion chains [17, 15, 16], which would facilitate

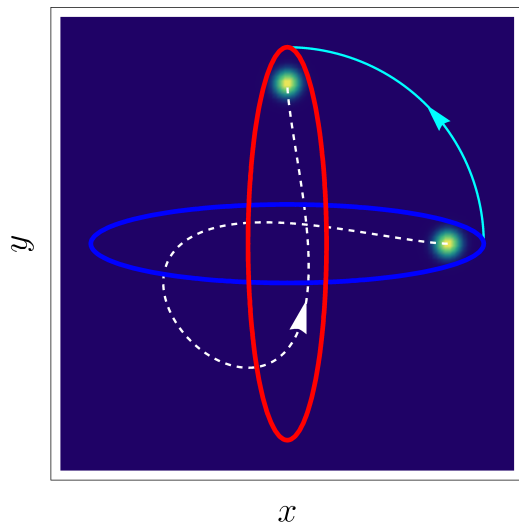


Figure 1. (Color online). Trap rotation in the lab frame (solid line arrow) and particle dynamics (dashed line arrow). The trap is at rest for $t < 0$ (horizontal ellipse); then it is rotated by $\pi/2$ from $t = 0$ to $t = T$; and finally it remains again at rest for $t > T$ (vertical ellipse). The trap rotation is designed such that the state at time T is the rotated version of the initial state, *for all possible -classical or quantum- initial states*. Just one of them -chosen arbitrarily- is depicted. The dashed line is the trajectory of the state center along the trap rotation process.

scalability in linear traps, and be useful to rearrange the chain, e.g. to locate a cooling ion at the right position in the chain [17]. Rotated states have other applications in sensing, metrology, and fundamental physics studies [18].

The treatment and transformations are done first in a classical setting. However, since we deal with a harmonic anisotropic trap the results can be translated into quantum mechanics rather directly. After setting the model in Sec. 2, the independent normal modes will be first defined and characterized by normal frequencies in Sec. 3. Section 4 analyzes the fast rotations that may be achieved at certain process times for configurations in which the normal frequencies are commensurate. The minimal time is identified, examples are given, and a stability analysis is carried out. Finally, Sec. 5 discusses some open questions.

2. Physical model

Our starting point is the Hamiltonian of a particle of mass m in a 2D anisotropic harmonic potential with axial (angular) frequencies ω_1 and ω_2 , which rotates around the z axis perpendicular to the trap plane by an angle θ with an angular velocity $\dot{\theta}$, see Fig. 1 (dots hereafter represent time derivatives). In the rotating frame of coordinates $\{\tilde{q}_1, \tilde{q}_2\}$ and momenta $\{\tilde{p}_1, \tilde{p}_2\}$ the Hamiltonian is given by, see Appendix A,

$$H = \frac{\tilde{p}_1^2}{2m} + \frac{\tilde{p}_2^2}{2m} + \frac{1}{2}m\omega_1^2\tilde{q}_1^2 + \frac{1}{2}m\omega_2^2\tilde{q}_2^2 - \dot{\theta}L_z, \quad (1)$$

where $L_z = \tilde{q}_1\tilde{p}_2 - \tilde{q}_2\tilde{p}_1$. H has the form of two harmonic oscillators coupled by an angular momentum L_z that accounts for the inertial effects [19].

By introducing the dimensionless coordinates and momenta

$$q_j = \sqrt{\frac{m\omega_j}{\hbar}}\tilde{q}_j, \quad p_j = \frac{\tilde{p}_j}{\sqrt{m\hbar\omega_j}}, \quad (2)$$

the Hamiltonian (1) can be written ($\hbar = 1$ hereafter) as

$$H = \frac{\omega_1}{2}(p_1^2 + q_1^2) + \frac{\omega_2}{2}(p_2^2 + q_2^2) - \dot{\theta} \left(\frac{1}{\eta}q_1p_2 - \eta q_2p_1 \right), \quad (3)$$

where $\eta = \sqrt{\omega_1/\omega_2}$.

This rotating frame Hamiltonian depends only on the angular velocity $\dot{\theta}$ as a control parameter. We shall consider, except in the final discussion, a constant rotation velocity, i. e., a linear-in-time angle $\theta(t) = \dot{\theta}t$ from $t = 0$ to $t = T$. Thus the Hamiltonian in the rotating frame is time independent during the rotation.

The Hamiltonian (3) can be written in compact matrix representation as the quadratic form

$$H = v^T A v, \quad (4)$$

where $v^T = (q_1, q_2, p_1, p_2)$ and A is the symmetric 4×4 matrix

$$A = \frac{1}{2} \begin{pmatrix} \omega_1 & 0 & 0 & -\frac{\dot{\theta}}{\eta} \\ 0 & \omega_2 & \eta\dot{\theta} & 0 \\ 0 & \eta\dot{\theta} & \omega_1 & 0 \\ -\frac{\dot{\theta}}{\eta} & 0 & 0 & \omega_2 \end{pmatrix}. \quad (5)$$

Our first goal is to find a transformation to a frame in which the corresponding effective Hamiltonian is uncoupled in both coordinates and momenta, or, using the four-dimensional matrix formalism, it is characterized by a diagonal matrix. To do so we will use the symplectic approach to canonical transformations.

3. Symplectic diagonalization

In the 4×4 matrix representation presented above, a canonical transformation will be defined by the transformation $v = SV$ to a new set of canonical coordinates $V^T = (Q_1, Q_2, P_1, P_2)$ provided S is a 4×4 symplectic matrix. A symplectic matrix S satisfies $S^T J S = J$, where J is the skew-symmetric matrix [19]

$$J = \begin{pmatrix} 0 & 0 & 1 & 0 \\ 0 & 0 & 0 & 1 \\ -1 & 0 & 0 & 0 \\ 0 & -1 & 0 & 0 \end{pmatrix}. \quad (6)$$

Note that its inverse is simply $J^{-1} = J^T = -J$. As well, $S^{-1} = J^{-1}S^T J$. 4×4 real symplectic matrices form the ten-dimensional symplectic group $Sp(4, \mathbb{R})$ [20]. Applying a symplectic (i. e., canonical) transformation to H amounts to rewrite it as

$$H = v^T A v = V^T (S^T A S) V. \quad (7)$$

Given the matrix A (5) we want to find a symplectic matrix $S \in Sp(4, \mathbb{R})$ so that $S^T A S$ is a diagonal matrix. Such a diagonalizing symplectic matrix S will always exist as long as A is a positive definite matrix. This result is known as Williamson's Theorem [21, 22, 23]. The positivity of A imposes an upper bound for the allowed rotation velocity in order to end up with an uncoupled effective Hamiltonian. In particular, the rotation velocity must satisfy

$$\dot{\theta} < \min(\omega_1, \omega_2). \quad (8)$$

For simplicity, and without loss of generality, we will consider $\omega_1 < \omega_2$ (or $0 < \eta < 1$) throughout this work. Therefore, the three (angular) frequencies in our model satisfy the conditions

$$\dot{\theta} < \omega_1 < \omega_2. \quad (9)$$

3.1. Constructing the S matrix

We will construct the S matrix after a four-step sequence of symplectic transformations.

i) The first transformation brings the matrix A (5) to a block diagonal form. This is achieved by the symplectic matrix

$$S_0 = \begin{pmatrix} 0 & 0 & -1 & 0 \\ 0 & 1 & 0 & 0 \\ 1 & 0 & 0 & 0 \\ 0 & 0 & 0 & 1 \end{pmatrix}, \quad (10)$$

which leads to

$$A_1 = S_0^T A S_0 = \frac{1}{2} \begin{pmatrix} \omega_1 & \eta \dot{\theta} & 0 & 0 \\ \eta \dot{\theta} & \omega_2 & 0 & 0 \\ 0 & 0 & \omega_1 & \frac{\dot{\theta}}{\eta} \\ 0 & 0 & \frac{\dot{\theta}}{\eta} & \omega_2 \end{pmatrix}. \quad (11)$$

This transformation is not a point transformation since S_0 mixes coordinates and momenta as already noted in [25].

ii) The second transformation diagonalizes one of the two blocks in A_1 . We choose the lower one in this case, the ‘‘momenta block’’. If $\omega_1 > \omega_2$ had been assumed, at this point the upper block should be diagonalized instead of the lower one. This transformation is performed by the symplectic matrix

$$S_1 = \begin{pmatrix} 1 & \frac{\dot{\theta}}{\sqrt{\omega_1 \omega_2}} & 0 & 0 \\ 0 & 1 & 0 & 0 \\ 0 & 0 & 1 & 0 \\ 0 & 0 & -\frac{\dot{\theta}}{\sqrt{\omega_1 \omega_2}} & 1 \end{pmatrix} \quad (12)$$

and leads to

$$A_2 = S_1^T A_1 S_1 = \frac{1}{2} \begin{pmatrix} \omega_1 & 2\eta\dot{\theta} & 0 & 0 \\ 2\eta\dot{\theta} & \frac{3\dot{\theta}^2 + \omega_2^2}{\omega_2} & 0 & 0 \\ 0 & 0 & \frac{\omega_1^2 - \dot{\theta}^2}{\omega_1} & 0 \\ 0 & 0 & 0 & \omega_2 \end{pmatrix}. \quad (13)$$

iii) The third step transforms the block that it is already diagonal (the lower block in our case) into the identity. This is achieved by the symplectic matrix

$$S_2 = \begin{pmatrix} \sqrt{\frac{\omega_1^2 - \dot{\theta}^2}{\omega_1}} & 0 & 0 & 0 \\ 0 & \sqrt{\omega_2} & 0 & 0 \\ 0 & 0 & \sqrt{\frac{\omega_1}{\omega_1^2 - \dot{\theta}^2}} & 0 \\ 0 & 0 & 0 & \frac{1}{\sqrt{\omega_2}} \end{pmatrix}, \quad (14)$$

which transforms A_2 into

$$A_3 = S_2^T A_2 S_2 = \frac{1}{2} \begin{pmatrix} \omega_1^2 - \dot{\theta}^2 & 2\dot{\theta}\sqrt{\omega_1^2 - \dot{\theta}^2} & 0 & 0 \\ 2\dot{\theta}\sqrt{\omega_1^2 - \dot{\theta}^2} & 3\dot{\theta}^2 + \omega_2^2 & 0 & 0 \\ 0 & 0 & 1 & 0 \\ 0 & 0 & 0 & 1 \end{pmatrix}. \quad (15)$$

The transformation requires $\omega_1 > \dot{\theta}$, which is consistent with Eq. (9).

iv) Finally, a (formal) rotation of an angle α brings the upper block to a diagonal form, leaving the lower block unaltered,

$$S_3 = \begin{pmatrix} \cos \alpha & -\sin \alpha & 0 & 0 \\ \sin \alpha & \cos \alpha & 0 & 0 \\ 0 & 0 & \cos \alpha & -\sin \alpha \\ 0 & 0 & \sin \alpha & \cos \alpha \end{pmatrix}, \quad (16)$$

with the angle of rotation α given by

$$\tan 2\alpha = \frac{4\dot{\theta}\sqrt{\omega_1^2 - \dot{\theta}^2}}{\omega_1^2 - \omega_2^2 - 4\dot{\theta}^2}. \quad (17)$$

This last transformation, leads to our objective, a diagonal matrix

$$A_4 = S_3^T A_3 S_3 = \frac{1}{2} \begin{pmatrix} \Omega_1^2 & 0 & 0 & 0 \\ 0 & \Omega_2^2 & 0 & 0 \\ 0 & 0 & 1 & 0 \\ 0 & 0 & 0 & 1 \end{pmatrix}, \quad (18)$$

where the $\Omega_{1,2}$ are the normal mode frequencies with squares

$$\begin{aligned} \Omega_1^2 &= \dot{\theta}^2 + \frac{\omega_1^2 + \omega_2^2}{2} - \frac{1}{2}\sqrt{8\dot{\theta}^2(\omega_1^2 + \omega_2^2) + (\omega_1^2 - \omega_2^2)^2}, \\ \Omega_2^2 &= \dot{\theta}^2 + \frac{\omega_1^2 + \omega_2^2}{2} + \frac{1}{2}\sqrt{8\dot{\theta}^2(\omega_1^2 + \omega_2^2) + (\omega_1^2 - \omega_2^2)^2}, \end{aligned} \quad (19)$$

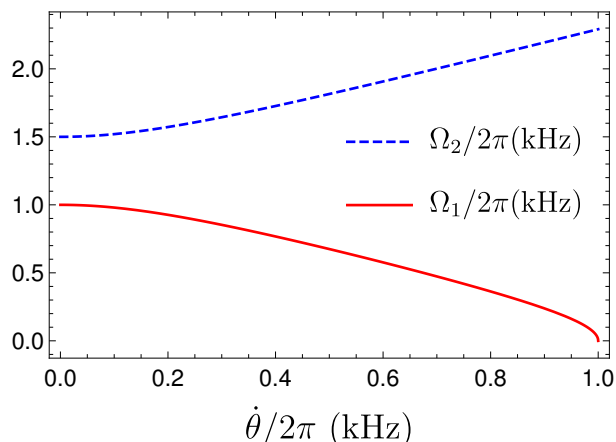


Figure 2. (Color online) Normal mode frequencies Ω_1 (red solid) and Ω_2 (blue dashed) as a function of the rotation angular velocity for axial frequencies $\omega_1 = 2\pi \times 1$ kHz and $\omega_2 = 1.5\omega_1$. There is a maximum allowed $\dot{\theta}$, when one of the normal mode frequencies (Ω_1 in this case) becomes complex $\dot{\theta}_{max} = \omega_1$, see Eq. (9). For a non-rotating trap ($\dot{\theta} = 0$), these frequencies are simply the axial frequencies $\omega_{1,2}$.

see a plot of these frequencies as a function of $\dot{\theta}$ in Fig. 2. These eigenfrequencies have been found before by Bialynicki-Birula using a different approach [24]. Our four-step method is sketched in [25], although the eigenfrequencies and explicit transformations were not given there.

3.2. Uncoupled Hamiltonian and normal modes

After the sequence of four different transformations, the symplectic matrix we were looking for can be written as (the product of symplectic matrices is symplectic)

$$S = S_0 S_1 S_2 S_3. \quad (20)$$

S diagonalizes the initial A matrix by the relation $A_4 = S^T A S$ and relates old coordinates and momenta in the rotating-frame and new coordinates and momenta in the transformed frame by the transformation $v = S V$ or

$$\begin{pmatrix} q_1 \\ q_2 \\ p_1 \\ p_2 \end{pmatrix} = S \begin{pmatrix} Q_1 \\ Q_2 \\ P_1 \\ P_2 \end{pmatrix}. \quad (21)$$

By inverting this relation, we can give explicit expressions for the new frame coordinates and momenta in terms of the original ones,

$$\begin{cases} Q_1 = q_2 \frac{\sqrt{\delta} \sin \alpha - \dot{\theta} \cos \alpha}{\sqrt{\delta \omega_2}} + p_1 \sqrt{\frac{\omega_1}{\delta}} \cos \alpha \\ Q_2 = q_2 \frac{\sqrt{\delta} \cos \alpha + \dot{\theta} \sin \alpha}{\sqrt{\delta \omega_2}} - p_1 \sqrt{\frac{\omega_1}{\delta}} \sin \alpha \\ P_1 = -q_1 \frac{\sqrt{\delta} \cos \alpha + \dot{\theta} \sin \alpha}{\sqrt{\omega_1}} + p_2 \sqrt{\omega_2} \sin \alpha \\ P_2 = q_1 \frac{\sqrt{\delta} \sin \alpha - \dot{\theta} \cos \alpha}{\sqrt{\omega_1}} + p_2 \sqrt{\omega_2} \cos \alpha \end{cases}, \quad (22)$$

with $\delta = \omega_1^2 - \dot{\theta}^2$, which makes clear that this is not a point transformation. The Hamiltonian written in normal-mode coordinates and momenta takes the simple form of two independent harmonic oscillators with normal frequencies $\Omega_{1,2}$,

$$H = v^T A v = V^T S^T A S V = V^T A_4 V = \frac{1}{2} (P_1^2 + P_2^2 + \Omega_1^2 Q_1^2 + \Omega_2^2 Q_2^2). \quad (23)$$

As discussed in Appendix B, these transformations are identical for a quantum Hamiltonian and can be related to quantum unitary transformations. Therefore, the Hamiltonian (23) can be quantized by substituting the generalized coordinate and momenta by the corresponding operators. Since the Hamiltonian is quadratic, we may equivalently rely on a phase-space description of the quantum state dynamics in Wigner representation. The dynamics of the Wigner function is governed by a classical Liouville equation; equivalently, a phase-space point is driven by classical Hamiltonian dynamics.

4. Fast rotations

4.1. Commensurate anisotropic oscillator

The time evolution generated by the Hamiltonian (23) is governed by two independent harmonic oscillators. In this frame, the corresponding classical trajectories will be given by Lissajous-like orbits, that will only be closed when the ratio between the $\Omega_{1,2}$ frequencies is a rational number, i. e., when they are commensurate. Let us suppose that $n_{1,2}$ are two integers ($1 \leq n_1 < n_2$). Then, if the condition

$$\frac{\Omega_2}{\Omega_1} = \frac{n_2}{n_1} \quad (24)$$

is satisfied, the full period of the dynamics is given by

$$T = \frac{2\pi n_1}{\Omega_1} = \frac{2\pi n_2}{\Omega_2}. \quad (25)$$

If a rotation is performed in a time T , the system will end up in the same initial state in the rotating frame: the first oscillator performs n_1 oscillations, and the second one n_2 full oscillations.

To perform a rotation of an angle $\theta_f = \dot{\theta}T$ (assuming an initial angle $\theta_i = 0$) at a constant angular velocity $\dot{\theta}$ in time T , the above relation may be written as

$$T = \frac{\theta_f}{\dot{\theta}} = \frac{2\pi n_1}{\Omega_1(\dot{\theta}, \omega_1, \omega_2)} = \frac{2\pi n_2}{\Omega_2(\dot{\theta}, \omega_1, \omega_2)}. \quad (26)$$

For some fixed values of θ_f , n_1 and n_2 , these equalities do not have a unique solution since there are two equations but three different parameters (rotation velocity $\dot{\theta}$, and frequencies ω_1 and ω_2). Using Eq. (26) we may write two of the frequencies in terms of a third one, for instance

$$\begin{aligned} \omega_1 &= \kappa_- \dot{\theta}, \\ \omega_2 &= \kappa_+ \dot{\theta}, \end{aligned} \quad (27)$$

ω_1	ω_2	$\dot{\theta}$	$T_{1,2} = \theta_f/\dot{\theta}$
$2\pi \times 1$ kHz	$2\pi \times 1.79$ kHz	$2\pi \times 0.23$ kHz	1.08 ms
$2\pi \times 2$ kHz	$2\pi \times 3.59$ kHz	$2\pi \times 0.46$ kHz	0.54 ms
$2\pi \times 5$ kHz	$2\pi \times 8.96$ kHz	$2\pi \times 1.16$ kHz	0.22 ms
$2\pi \times 10$ kHz	$2\pi \times 17.93$ kHz	$2\pi \times 2.32$ kHz	0.11 ms

Table 1. Some numerical values of the trapping frequencies ω_1 and ω_2 , rotation angular velocity $\dot{\theta}$ and time duration T of the rotation operation calculated according to Eqs. (26-29). $\theta_f = \pi/2$, $n_1 = 1$, and $n_2 = 2$.

where

$$\kappa_{\pm} = \left(-1 + \frac{2\pi^2\delta_+}{\theta_f^2} \pm \frac{2\sqrt{\pi^4\delta_-^2 - 2\pi^2\delta_+\theta_f^2 + \theta_f^4}}{\theta_f^2} \right)^{1/2} \quad (28)$$

with $\delta_{\pm} = n_1^2 \pm n_2^2$. Once one of the frequencies is fixed, the remaining two will be determined by Eq. (27). In the following, the value of the smallest axial frequency ω_1 will be fixed, but a similar analysis could be done if any of the two remaining ones is fixed: also of interest is the setting where ω_1 and ω_2 are given, i.e., we do not assume that their values can be controlled. Then $\dot{\theta}$ for different n_1, n_2 should be adjusted to satisfy the last equality in Eq. (26). Since T is fixed by the last two ratios in Eq. (26), only a set of discrete values of θ_f are allowed in this scenario.

For a given value of ω_1 , relation (27) determines $\dot{\theta}$ and ω_2 , and using Eq. (26) the time duration of the rotation operation is

$$T_{n_1, n_2} = \frac{\kappa_- \theta_f}{\omega_1}, \quad (29)$$

which, for some fixed values of ω_1 and θ_f , is just a function of the integers n_1 and n_2 . See some numerical values of $T_{1,2}$ for a $\pi/2$ rotation in Table 1.

4.2. Fast rotations

In principle, the values of n_1 and n_2 can be chosen arbitrarily as long as $n_1 < n_2$: The time duration of a given rotation (for given θ_f and ω_1) will be completely determined by the factor κ_- . As it is shown in Fig. 3a-b, the fastest possible rotation (minimum value of κ_-) is found with the values $n_1 = 1$ and $n_2 \rightarrow \infty$. This means that the minimum rotation time T_{\min} corresponds to a single oscillation of the first (slow) normal mode oscillator and to infinitely many oscillations of the second one,

$$T_{\min} = T_{1, \infty} = \sqrt{\frac{\theta_f^2 + 4\pi^2}{\omega_1^2}}. \quad (30)$$

This minimal time corresponds to the $\omega_1 \ll \omega_2$ limit (i. e., an infinitely narrow trap) as shown in Fig. 3c.

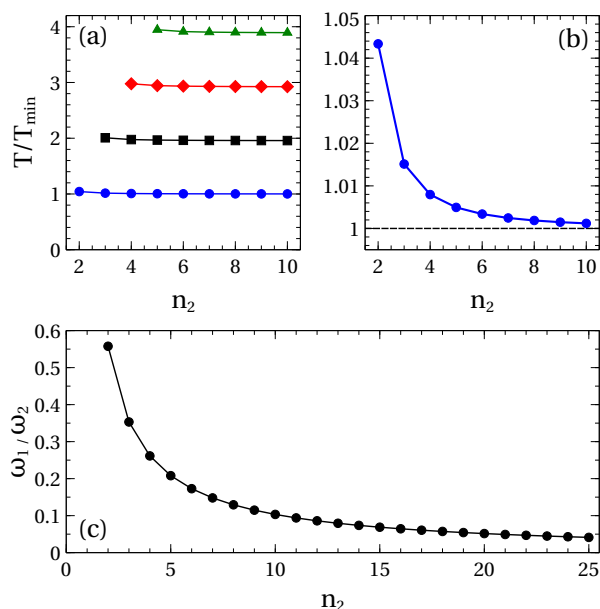


Figure 3. (Color online) (a) Time T to perform a rotation of $\pi/2$ without final excitation as a function of n_2 for different values of n_1 : $n_1 = 1$ blue circles, $n_1 = 2$ black squares, $n_1 = 3$ red diamonds and $n_1 = 4$ green triangles. The fastest possible rotation corresponds to $n_1 = 1$ and $n_2 \rightarrow \infty$. (b) Closer look at the $n_1 = 1$ series. (c) Ratio between axial frequencies $\omega_1/\omega_2 = \kappa_-/\kappa_+$ for $n_1 = 1$. As n_2 increases the trap gets narrower. The fastest possible rotation, at the $n_2 \rightarrow \infty$ limit, occurs for an infinitely narrow trap $\omega_1 \ll \omega_2$.

Of course this limit is an idealization and in practice ω_2 will have some maximal value. To illustrate features of a generic case ($n_2 \neq \infty$) we choose $n_1 = 1$ and $n_2 = 2$ in numerical calculations.

4.3. Time evolution of states and observables

In the reference system of the normal modes, $\{Q_1, Q_2\}$, a general wave function takes the form

$$\psi(Q_1, Q_2, t) = \sum_{j=0}^{\infty} \sum_{j'=0}^{\infty} c_{jj'} \phi_j^{(1)}(Q_1) e^{-i\Omega_1(j+\frac{1}{2})t} \phi_{j'}^{(2)}(Q_2) e^{-i\Omega_2(j'+\frac{1}{2})t}, \quad (31)$$

where the $c_{jj'}$ are constant coefficients set by the initial conditions and $\phi_j^{(1,2)}(Q_{1,2})$ are the usual stationary eigenfunctions of the harmonic oscillators. If the rotation continues indefinitely, at a time $t + T$ with T given in Eq. (25), one gets

$$\begin{aligned} \psi(Q_1, Q_2, t + T) &= \sum_{j=0}^{\infty} \sum_{j'=0}^{\infty} c_{jj'} \phi_j^{(1)}(Q_1) e^{-i\Omega_1(j+\frac{1}{2})(t+\frac{2\pi n_1}{\Omega_1})} \\ &\quad \times \phi_{j'}^{(2)}(Q_2) e^{-i\Omega_2(j'+\frac{1}{2})(t+\frac{2\pi n_2}{\Omega_2})} \\ &= (-1)^{n_1+n_2} \psi(Q_1, Q_2, t), \end{aligned} \quad (32)$$

i. e., the wave function one period T earlier, with an overall phase that depends on $n_1 + n_2$. The quantum system is said to experience “exact revivals” at intervals of T [26]. Here we are interested in setting $t = 0$ and the corresponding revival at T .

In the numerical examples the dynamics is solved entirely in a truncated Fock space for the interaction-free part (two harmonic oscillators) which is enlarged until convergence is achieved.

4.3.1. Periodic orbits in the rotating frame In the normal-mode frame, the classical trajectories or corresponding center of a wavepacket describe closed Lissajous orbits for commensurate normal frequencies. In the rotating frame we find also corresponding closed orbits.

To visualize them let us suppose that the system is initially in the two-mode coherent state $|\psi(0)\rangle = |\alpha_1, \alpha_2\rangle$. The state $|\alpha_1, \alpha_2\rangle$ may be expanded in terms of number states of the harmonic oscillators with frequencies $\omega_{1,2}$,

$$|\alpha_1, \alpha_2\rangle = e^{-\frac{1}{2}(|\alpha_1|^2 + |\alpha_2|^2)} \sum_{n_1, n_2=0}^{\infty} \frac{\alpha_1^{n_1} \alpha_2^{n_2}}{\sqrt{n_1! n_2!}} |n_1, n_2\rangle,$$

with $\alpha_j = |\alpha_j| e^{i\varphi}$ and

$$\langle q_1, q_2 | n_1, n_2 \rangle = \frac{e^{-\frac{q_1^2 + q_2^2}{2}} H_{n_1}(q_1) H_{n_2}(q_2)}{\sqrt{2^{n_1 + n_2} n_1! n_2! \pi}}, \quad (33)$$

where $H_n(q)$ is the n th order Hermite polynomial. The time-evolved two-mode coherent state in coordinate representation will be given by the wave function

$$\langle q_1, q_2 | \psi(t) \rangle = \langle q_1, q_2 | e^{-iHt} | \alpha_1, \alpha_2 \rangle \quad (34)$$

By integrating the probability density over a full period T ,

$$\mathcal{P}(q_1, q_2) = \int_0^T |\langle q_1, q_2 | \psi(t) \rangle|^2 dt, \quad (35)$$

a track of the wave-packet is found, see Fig. 4, which is more intense where the motion is slow. The center of the wave-packet follows the classical closed Lissajous-like orbits, ending in its initial configuration after a full rotation is performed.

4.3.2. Mean number of excitations, survival probability. We will now consider the mean vibrational number as a function of time in the rotating frame,

$$\langle N(t) \rangle = \langle \psi(t) | a_1^\dagger a_1 + a_2^\dagger a_2 | \psi(t) \rangle, \quad (36)$$

where the creation and annihilation operators in each direction are defined in terms of position and momentum operators as usual,

$$a_j = \frac{1}{\sqrt{2}}(\hat{q}_j + i\hat{p}_j), \quad a_j^\dagger = \frac{1}{\sqrt{2}}(\hat{q}_j - i\hat{p}_j), \quad (37)$$

for $j = 1, 2$. In the first column of Fig. 5, the time evolution of the mean number of excitations during $\pi/2$ rotations designed without final excitation using the first row

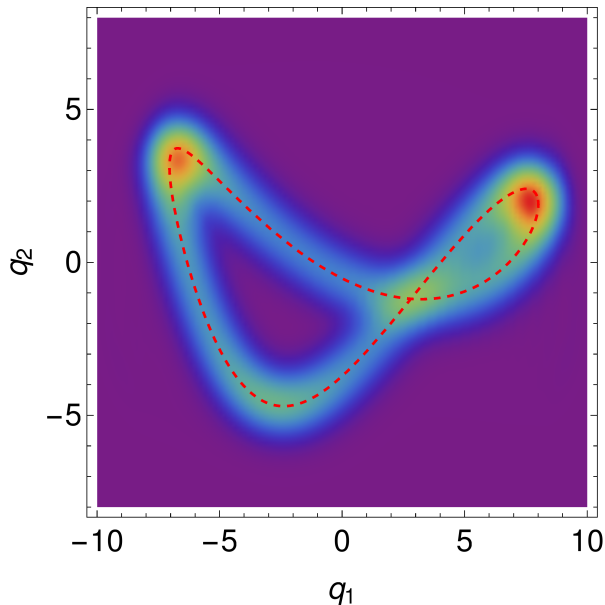


Figure 4. (Color online) Wavepacket track $\mathcal{P}(q_1, q_2)$ of the two mode coherent state $|\alpha_1, \alpha_2\rangle$ for the values (initial conditions) $\alpha_1 = 8/\sqrt{2}$ and $\alpha_2 = 2/\sqrt{2}$ during a rotation of an angle of $\pi/2$. Red dashed line: corresponding classical trajectory with initial conditions $q_1(0) = \sqrt{2}|\alpha_1| = 8$, $q_2(0) = \sqrt{2}|\alpha_2| = 2$ and $p_1(0) = p_2(0) = 0$. The trap and rotation parameters are those in the first row of Table 1. Dimensionless spatial coordinates q_1 and q_2 have been used as explained in the text.

of Table 1 ($n_1 = 1, n_2 = 2$) is shown for different initial states: the ground state of the non-rotating trap, an entangled state, and a coherent state. Interestingly, Fig. 5 (first column) demonstrates that the mean excitation can actually decrease, at least transiently, with respect to the initial value. Of course for all states the final value coincides with the initial value.

The rotation process has been chosen so that the survival probability in the rotating frame $P(t) = |\langle \psi(t) | \psi(0) \rangle|^2$ satisfies the condition $P(0) = P(T)$, due to commensurability. In the second column of Fig. 5, the probability of finding the system in its initial state is calculated for different initial quantum states. The revivals are seen clearly in all three cases. The survival of the coherent and entangled states decays at intermediate times much more severely than the one for the ground state. Indeed, a classical particle set initially at rest at the bottom of the trap would not be affected by the trap rotation.

4.4. Stability

As already pointed out in Sec. 4.2, the fastest allowed rotations are found for $n_1 = 1$ and $n_2 \gg 1$, which imply very narrow quasi-1D traps with $\omega_2 \gg \omega_1$. However, fast rotations come with a price, since as n_2 increases the ideal result becomes more unstable. This can be intuitively understood: for larger n_2 the second normal oscillator oscillates faster so

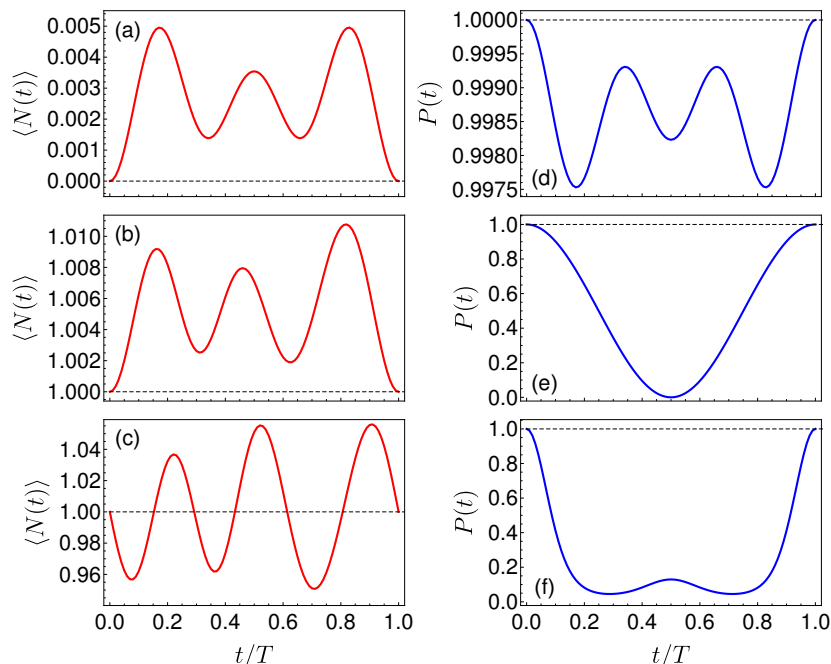


Figure 5. (Color online) Time evolution of different observables during a $\theta_f = \pi/2$ rotation. In the left column the evolution of the average number of excitations $\langle N(t) \rangle$ is plotted as a function of time, while in the second the survival probability $P(t) = |\langle \psi(t) | \psi(0) \rangle|^2$ of finding the system in its initial state (in the rotating frame) is plotted. Different initial states are considered for each figure: In (a) and (d), the initial state is the ground state of a 2D oscillator $|\nu(0)\rangle = |0, 0\rangle$ with $\langle N(0) \rangle = 0$. In (b) and (e), the initial state is an entangled state $|\nu(0)\rangle = \frac{1}{\sqrt{2}}(|0, 1\rangle + |1, 0\rangle)$ with $\langle N(0) \rangle = 1$. In (c) and (f), the initial state is a coherent state $|\nu(0)\rangle = |\alpha_1, \alpha_2\rangle$ with $\alpha_1 = \alpha_2 = 1/\sqrt{2}$ (i. e., a minimum uncertainty wave packet centered at $q_1 = q_2 = 1$ with mean number of excitations $\langle N(0) \rangle = |\alpha_1|^2 + |\alpha_2|^2 = 1$). Trap and rotation parameters are those in the first row of Table 1.

it is easier to miss the exact final state due to some small timing error. This is confirmed in Fig. 6, which depicts the survival probability as a function ϵ , a small deviation from the nominal operation time T . For larger n_2 the survival becomes less robust.

This effect can be quantified by approximating the survival probability to second order in ϵ as

$$P(T + \epsilon) \approx 1 - \Delta H^2 \epsilon^2 \quad (38)$$

with

$$\Delta H^2 = \langle \psi(0) | H^2 | \psi(0) \rangle - \langle \psi(0) | H | \psi(0) \rangle^2. \quad (39)$$

ΔH^2 depends on the considered initial state as Fig. 5 (right column) illustrates. The survival probability of the ground state, in particular, decays with ϵ^2 at a rate

$$\Delta H^2 = \frac{\dot{\theta}^2 (\omega_1 - \omega_2)^2}{4\omega_1\omega_2}, \quad (40)$$

which, for a given ω_1 , increases for faster rotations (larger $\dot{\theta}$ and ω_2).

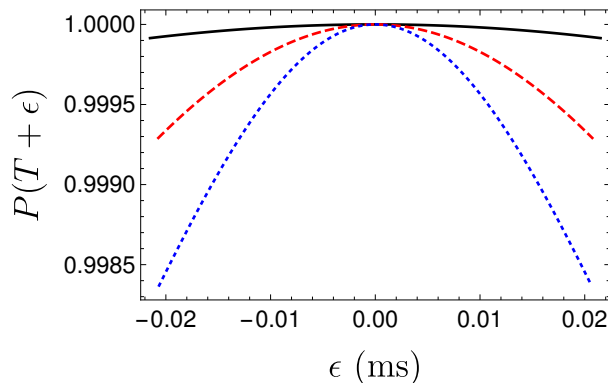


Figure 6. (Color online) Stability when the rotation lasts $T + \epsilon$. The survival probability is plotted as a function of ϵ for the example shown in Fig. 5d ($\pi/2$ rotation of the ground state) for $n_1 = 1$ and different integer values of n_2 : $n_2 = 2$ (black-solid line), $n_2 = 5$ (red-dashed line), and $n_2 = 10$ (blue-dotted line).

4.5. Comparison with slow adiabatic rotations

An example to see how much faster the process may be compared to a slow adiabatic rotation is depicted in Fig. 7. The trap is set with the angular frequencies fixed for a $n_1 = 1$, $n_2 = 2$ configuration and a $\theta_f = \pi/2$ rotation, see the first line in Table 1. The time $T = 1.08$ ms satisfying (26) is the scale used to compare the final error to find the ideal rotated state by keeping ω_1 and ω_2 fixed but varying the final process time t_f and therefore the rotation speed as $\dot{\theta} = \theta_f/t_f$. We use an initial state of interest in a quantum information scenario, $|0, 1\rangle$. This state is initially stationary and will remain stationary after the ideal rotation that takes a time $t_f = T$, which gives by construction a perfect fidelity. For some special larger times the conditions where t_f is an integer number of both normal-mode periods are almost (but not exactly) fulfilled. We note that a 10^{-4} error value for the upper envelop of the error curve needs about $t_f > 60T$.

5. Discussion

Controlling the motion of quantum particles is needed to manipulate them for fundamental science studies and to develop different quantum technologies. In particular, operations which are fast, robust, and do not leave residual excitations are typically preferred. Here we focused on rotating arbitrary states of a single particle in an anisotropic harmonic trap using the rotation speed and rotation time as the only control parameters. By “rotating” a state here we mean to end at a time $t = T$ with a particle and trap configuration which is identical to the one at time $t = 0$ but rotated by some angle θ_f in the laboratory frame. As an inverse problem, even such a simple system and operation involves considerable complexities. Since normal modes cannot be found by a point transformation, we have first performed a non point (but canonical) transformation to find the normal modes for constant rotation speed. Based on the

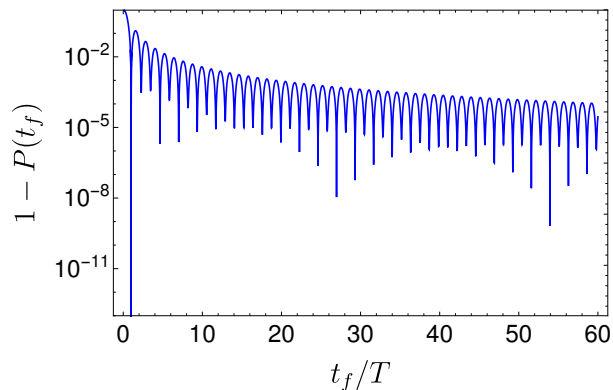


Figure 7. (Color online) One minus the survival probability at final time t_f (logarithmic scale) in the rotating frame for a $\theta_f = \pi/2$ rotation versus the scaled total process time t_f/T , with $T = 1.08$ ms being the process time using our fast protocol. The initial state is the excited state $|0, 1\rangle$. The trap frequencies ω_1 and ω_2 are fixed with the values in the first row of Table 1.

normal mode analysis we apply a protocol in which any initial state becomes its rotated version in the final trap. Minimal times are found and a stability analysis with respect to time errors is performed.

We may envision several worthwhile and natural extensions of this work such as considering anharmonicities, two or more interacting particles in the trap, or, to achieve further flexibility in the rotation times, time-dependent rotation speeds $\dot{\theta}(t)$. This time-dependence makes the $A(t)$ matrix in the Hamiltonian of the rotating frame time dependent, and following the steps in the main text and Appendix B we may perform a time-dependent symplectic transformation and find that the interaction picture effective Hamiltonian will be given by $H_I = v^T[S^T(A - \dot{G})S]v$, where G is the real symmetric matrix that generates the symplectic matrix S , $S = e^{2JG}$, see Appendix B. Finding the time-dependent symplectic transformation S that makes the 4×4 matrix $A' = S^T(A - \dot{G})S$ diagonal is a challenging open question, since it involves a highly non-linear system of coupled differential equations to determine the elements of G (and therefore S).

We cannot fail to point out an analogy between the structure of A' and the effective Hamiltonian used in superadiabatic iterations to achieve shortcuts [27, 28]. If S is set to diagonalize A , rather than the whole matrix A' , two uncoupling strategies are: to ignore the inertial term $\mathcal{I} = -S^T\dot{G}S$ because it is small (this is analogous to an adiabatic approximation), or to compensate it exactly with $-\mathcal{I}$ (this is analogous to counter-diabatic driving). However implementing such a compensating term is often difficult in practice, in this case it implies crossed operator terms. A third route is to apply the next ‘‘superadiabatic’’ iteration, i.e., to find an S' that makes $S'^T A' S'$ diagonal, which produces a term $\mathcal{I}' = -S'^T \dot{G} S'$ in the new Hamiltonian. Further iterations would repeat the same scheme but they do not need to converge so there may be an optimal iteration. Alternatively the coupling term may be approximated to achieve convergence [29]. All

this is very intriguing and will be explored elsewhere.

Acknowledgments

We are grateful to K. Takahashi for discussions in early stages of the work. This work was supported by the Basque Country Government (Grant No. IT986-16) and PGC2018-101355-B-I00 (MCIU/AEI/FEDER,UE).

Appendix A. Laboratory frame

The Hamiltonian for a particle of mass m in a two-dimensional anisotropic harmonic potential with axial frequencies ω_1 and ω_2 and with a time varying orientation angle $\theta(t)$ (i. e., which is rotating around the z axis with angular velocity $\dot{\theta}(t)$) is given in laboratory $\{x, y\}$ frame by

$$H_{\text{lab}} = \frac{p_x^2}{2m} + \frac{p_y^2}{2m} + \frac{m\omega_1^2}{2} [x \cos \theta(t) + y \sin \theta(t)]^2 + \frac{m\omega_2^2}{2} [-x \sin \theta(t) + y \cos \theta(t)]^2. \quad (\text{A.1})$$

Defining the rotated coordinates and momenta by the relations

$$\begin{pmatrix} \tilde{q}_1 \\ \tilde{q}_2 \end{pmatrix} = R(t) \begin{pmatrix} x \\ y \end{pmatrix}; \quad \begin{pmatrix} \tilde{p}_1 \\ \tilde{p}_2 \end{pmatrix} = R(t) \begin{pmatrix} p_x \\ p_y \end{pmatrix} \quad (\text{A.2})$$

with $R(t)$ being the usual rotation matrix

$$R(t) = \begin{pmatrix} \cos \theta(t) & \sin \theta(t) \\ -\sin \theta(t) & \cos \theta(t) \end{pmatrix}, \quad (\text{A.3})$$

the new Hamiltonian is given by

$$H = \frac{\tilde{p}_1^2}{2m} + \frac{\tilde{p}_2^2}{2m} + \frac{1}{2}m\omega_1^2\tilde{q}_1^2 + \frac{1}{2}m\omega_2^2\tilde{q}_2^2 - \dot{\theta}L_z, \quad (\text{A.4})$$

with $L_z = \tilde{q}_1\tilde{p}_2 - \tilde{q}_2\tilde{p}_1$. This last term, which couples coordinates and momenta, accounts for the inertial effects that arise due to the time-dependent canonical transformation applied.

Appendix B. Quantum unitary transformations

It is also instructive to set a quantum description by means of a unitary transformation of the Hamiltonian. As it is well known from group theory, the generators of symplectic matrices are symmetric matrices in the sense that any symplectic matrix S can be written in terms of its generator G as $S = e^{2JG}$, G being a symmetric matrix and J the symplectic matrix (6). Let us define the unitary operator

$$\mathcal{U} = e^{iv^T G v}, \quad (\text{B.1})$$

where v^T is now regarded as a vector of operators $v^T = (\hat{q}_1, \hat{q}_2, \hat{p}_1, \hat{p}_2)$. The unitarily transformed, interaction picture Hamiltonian will be given by

$$H_I = \mathcal{U}H\mathcal{U}^\dagger + i\dot{\mathcal{U}}\mathcal{U}^\dagger, \quad (\text{B.2})$$

where the last term arises due to the possible time dependence of the unitary transformation. For a quadratic Hamiltonian with the form $H = v^T A v$, see Eq. (4), and the unitary operator \mathcal{U} defined by (B.1), it can be shown that the above effective Hamiltonian is given by

$$H_I = v^T \left[S^T \left(A - \dot{G} \right) S \right] v. \quad (\text{B.3})$$

Details of this calculation are given in Appendix C.

In a time independent scenario, where $\dot{G} = \dot{S} = 0$, we have an uncoupled (i. e., without cross terms) effective interaction picture Hamiltonian

$$H_I = v^T (S^T A S) v \quad (\text{B.4})$$

since $S^T A S$ is a diagonal matrix as shown in Sec. 3. Indeed, the inverse unitary transformation $\mathcal{U}^\dagger(\dots)\mathcal{U}$ maps all the components v_j to V_j ,

$$\mathcal{U}^\dagger v_j \mathcal{U} = (S^{-1}v)_j = V_j, \quad (\text{B.5})$$

so that H is recovered,

$$H = \mathcal{U}^\dagger H_I \mathcal{U} = V^T (S^T A S) V = v^T A v. \quad (\text{B.6})$$

In summary, the same symplectic transformation that diagonalizes the classical Hamiltonian matrix provides as well a quantum Hamiltonian written as a sum of quadratic operators without cross terms.

If the symplectic transformation S depends on time, the extra term $-v^T (S^T \dot{G} S) v$ has to be included in the effective Hamiltonian to account for the inertial effects. For a time dependent transformation, one would have to symplectically diagonalize the full matrix $A - \dot{G}$.

Appendix C. Detailed calculation of Eq. (B.3)

Let \mathcal{A} and \mathcal{B} be two real symmetric matrices. Taking into account that the position-momentum commutators $[q_j, p_k] = i\delta_{jk}$ can be summarized as $[v_j, v_k] = iJ_{jk}$, one can find the relation

$$\sum_{n=0}^{\infty} \frac{[v^T \mathcal{B} v, v^T \mathcal{A} v]_n}{n!} = v^T (e^{2i\mathcal{B}J} \mathcal{A} e^{-2iJ\mathcal{B}}) v, \quad (\text{C.1})$$

where $[v^T \mathcal{B} v, v^T \mathcal{A} v]_n = [v^T \mathcal{B} v, v^T \mathcal{B} v, \dots, [v^T \mathcal{B} v, v^T \mathcal{A} v]]$ denotes the n th nested commutator between the involved operators. Using this result, the two terms in the effective Hamiltonian (B.2) will be calculated separately:

(i) The first term $\mathcal{U}H\mathcal{U}^\dagger$ can be calculated using the Baker-Campbell-Hausdorff (BCH) formula and the previous result (C.1) to sum the series expansion. For the

unitary operator defined in (B.1) and a Hamiltonian with the form (4) we have

$$\begin{aligned} \mathcal{U}H\mathcal{U}^\dagger &= e^{iv^T Gv} (v^T Av) e^{-iv^T Gv} = \sum_{n=0}^{\infty} \frac{[iv^T Gv, v^T Av]_n}{n!} \\ &= v^T (e^{-2GJ} A e^{2JG}) v = v^T (S^T A S) v. \end{aligned} \quad (\text{C.2})$$

(ii) To calculate the second term $i\dot{\mathcal{U}}\mathcal{U}^\dagger$, we must be careful when computing the time derivative of \mathcal{U} , since it involves not-commuting operators [30],

$$\begin{aligned} i\dot{\mathcal{U}}\mathcal{U}^\dagger &= i \sum_{n=0}^{\infty} \frac{[iv^T Gv, iv^T \dot{G}v]_n}{n!} = -v^T (e^{-2GJ} \dot{G} e^{2JG}) v \\ &= -v^T (S^T \dot{G} S) v. \end{aligned} \quad (\text{C.3})$$

Here, again, Eq. (C.1) has been used to sum the series expansion.

The sum of these two terms leads finally to the interaction picture effective Hamiltonian (B.3)

$$H_I = \mathcal{U}H\mathcal{U}^\dagger + i\dot{\mathcal{U}}\mathcal{U}^\dagger = v^T \left[S^T (A - \dot{G}) S \right] v. \quad (\text{C.4})$$

References

- [1] E. Torrontegui et al., *Advances in atomic, molecular, and optical physics* **62**, 117 (2013).
- [2] D. Guéry-Odelin, A. Ruschhaupt, A. Kiely, E. Torrontegui, S. Martínez-Garaot, and J. G. Muga, *Review of Modern Physics* (2019), accepted, arXiv:1904.08448.
- [3] M. Palmero, R. Bowler, J. P. Gaebler, D. Leibfried, and J. G. Muga, *Phys. Rev. A* **90**, 053408 (2014).
- [4] M. Palmero, E. Torrontegui, D. Guéry-Odelin, and J. G. Muga, *Phys. Rev. A* **88**, 053423 (2013).
- [5] M. Palmero, S. Martínez-Garaot, J. Alonso, J. P. Home, and J. G. Muga, *Phys. Rev. A* **91**, 053411 (2015).
- [6] M. Palmero, S. Martínez-Garaot, U. G. Poschinger, A. Ruschhaupt, and J. G. Muga, *New J. Phys.* **17**, 093031 (2015).
- [7] X. J. Lu, M. Palmero, A. Ruschhaupt, X. Chen, and J. G. Muga, *Phys. Scr.* **90**, 074038 (2015).
- [8] M. Palmero, S. Wang, D. Guéry-Odelin, Jr-Shin Li, and J. G. Muga, *New J. Phys.* **18**, 043014 (2016).
- [9] M. Palmero, S. Martínez-Garaot, D. Leibfried, D. J. Wineland, and J. G. Muga, *Phys. Rev. A* **95**, 022328 (2017).
- [10] I. Lizuain, M. Palmero, J. G. Muga, *Phys. Rev. A* **95**, 022130 (2017).
- [11] S. Masuda and S. A. Rice, *J. Phys. Chem. B* **119**, 11079 (2015).
- [12] A. L. Fetter, *Rev. Mod. Phys.* **81**, 647 (2009).
- [13] J. Dalibard, F. Gerbier, G. Juzeliūnas, and P. Öhberg, *Rev. Mod. Phys.* **83**, 1523 (2011).
- [14] J. M. Amini, H. Uys, J. H. Wesenberg, S. Seidelin, J. Britton, J. J. Bollinger, D. Leibfried, C. Ospelkaus, A. P. VanDevender, and D. J. Wineland, *New J. Phys.* **12**, 033031 (2010).
- [15] W. K. Hensinger et al 2006 *Appl. Phys. Lett.* **88**, 034101 (2006).
- [16] R. B. Blakestad, A. P. VanDevender, C. Ospelkaus, J.M. Amini, J. Britton, D. Leibfried, and D. J. Wineland, *Phys. Rev. Lett.* **102**, 153002 (2009).
- [17] F. Splatt, M. Harlander, M. Brownutt, F. Zähringer, R. Blatt, and W. Hänsel, *New J. Phys.* **11**, 103008 (2006).
- [18] E. Urban, N. Glikin, S. Mouradian, K. Krimmel, B. Hemmerling, and H. Haeffner, arXiv:1903.05763v1
- [19] H. Goldstein, C. Poole, and J. Safko, *Classical Mechanics*, 3rd Ed, Addison-Wesley (2001).
- [20] R. Simon, *Phys. Rev. Lett.* **84**, 2726 (2000).
- [21] J. Williamson, *Am. J. Math.* **58**, 141(1936).
- [22] S. Pirandola, A. Serafini, and S. Lloyd, *Phys. Rev. A.* **79**, 052327 (2009).
- [23] M. de Gosson, *Symplectic Geometry and Quantum Mechanics* (Springer, Basel, 2006).
- [24] I. Bialynicki-Birula and Z. Bialynicka-Birula, *Phys. Rev. Lett.* **78**, 2539 (1997).
- [25] F. Leyraz, V. I. Man'ko, and T. H. Seligman, *Phys. Lett. A* **210**, 26 (1996).
- [26] K. Razi Naqvi and S. Waldenstrøm, *Phys. Scr.* **62**, 12 (2000).
- [27] M. Demirplak and S. A. Rice, *J. Chem. Phys.* **129**, 154111 (2008).
- [28] S. Ibáñez, X. Chen, and J. G. Muga, *Phys. Rev. A* **87**, 043402 (2013).
- [29] L. S. Theis, F. Motzoi, S. Machnes, and F. K. Wilhelm, *EPL (Europhysics Letters)* **123**, 60001 (2018).
- [30] B. C. Hall, “Lie groups, Lie algebras, and representations: An elementary introduction”, *Graduate Texts in Mathematics*, Springer (2015)